



# Polarization spectroscopy to determine alignment depolarization of the $^{133}\text{Cs } 6p^2P_{3/2}$ atoms using a pump-probe laser technique

S. Burçin Bayram \*, Prakash Koirala

Department of Physics, Miami University, 620 E. Spring Street, Oxford, OH 45056, USA

## ARTICLE INFO

### Article history:

Received 5 August 2008

Received in revised form 20 December 2008

Accepted 21 December 2008

### PACS:

32.00.00

32.90.+a

32.50.+d

### Keywords:

Spectroscopy

Atom-atom collisions

Polarization

## ABSTRACT

We have experimentally investigated alignment depolarization cross section of the excited  $J = 3/2$   $^{133}\text{Cs}$  atoms, by collisions with ground level krypton atoms, from a two-photon two-color linear polarization spectra. To measure the linear polarization degree of the  $6s^2S_{1/2} \rightarrow 6p^2P_{3/2} \rightarrow 10s^2S_{1/2}$  double-resonance transition, a nanosecond pulse pump-probe laser technique was employed. Alignment was optically induced by linear polarization of the pump laser. By analyzing the intensity of the cascade fluorescence signal, monitored from the  $9p^2P_{1/2} \rightarrow 6s^2S_{1/2}$  transition at 361.73 nm, in the presence of Kr pressures ranging from 7 mbar to 133 mbar a depolarization cross section value of  $294 (45) \text{ \AA}^2$  is obtained.

Published by Elsevier B.V.

## 1. Introduction

Measurements of collisional depolarization cross sections play important role to gain valuable information about the interaction between neutral atoms and rare gases [1–5]. In particular, dynamical information about the state multipoles, accurate description of the intermediate levels of the collision complex, accuracy of anisotropic molecular potentials, energy and charge transfer processes can be deduced from the investigation of atom-atom collisions [6–9]. Although the study of collision dynamics is not new, significant advances in techniques for laser cooling and trapping of atoms, molecules and ions has enormously increased the interest in this area of research [10,11]. For example, collisions involving cold Rydberg atoms has been a great interest in many fields of research due to the interesting properties of these atoms in astrophysical and laboratory plasmas [12–14]. Also, collisional depolarization cross section measured for colliders as rare gas or molecules is very important to the applications of laser induced fluorescence, atmospheric and combustion monitoring [15].

Optically induced anisotropic medium in atomic, molecular and optical systems has always been an interesting phenomena to

study. Study of anisotropy offers a large variety of applications such as polarization control of inhomogeneous media [16] including recent exciting applications to the study of radiative transport in ultracold atomic medium [17] and invisibility cloaking metamaterials [18]. Also, creating and probing anisotropic angular momentum distribution, *i.e.* orientation and alignment, in physical and chemical systems is important for the determination of correlation between relevant vector quantities. In particular, the importance of angular momentum polarization and vector correlations such as laser polarization, molecule transition moment, and angular distribution are shown to be essential for testing classical and quantum mechanical concepts concerning the dynamics of matter on a microscopic level [19]. To describe the anisotropic angular momentum distribution in the excited level by means of absorption or emission of polarized light a spherical tensor formalism has been developed [20,21]. From the spherical tensor formalism, atomic polarizations has been expressed in terms of the irreducible tensor components of the atomic density matrix, or the components of state multipoles. In this work, optically induced alignment in the  $6p^2P_{3/2}$  level cesium atoms was created from linearly polarized light and a two-photon two-color linear polarization spectrum was measured. From the spectroscopic measurements, collisional depolarization cross section (disalignment) in the  $^2P_{3/2}$  level cesium atoms in collision with the ground level krypton atoms at various pressures was extracted. We used a double-resonance pump-probe laser technique for the  $6s^2S_{1/2} \rightarrow 6p^2P_{3/2} \rightarrow 10s^2S_{1/2}$

\* Corresponding author. Tel.: +1 513 529 5630; fax: +1 513 529 5629.

E-mail address: [bayramsb@muohio.edu](mailto:bayramsb@muohio.edu) (S. Burçin Bayram).

transition. In the technique, the first photon optically induces an alignment in the excited level while the second photon senses the alignment during the excitation to the final level. This technique permits selective excitation to the Zeeman sublevels and direct measurement of the time evolution of the alignment in the excited level, both of which are difficult to study by other means. It is very powerful to use density matrix formalism in order to define analysis of depolarization cross section in the excited level alkali colliding with a rare-gas perturber. Thus, in this report, density matrix formalism with expansion in irreducible tensor operators are briefly introduced for the description of linear polarization spectrum. Experimental investigations of disalignment cross section in the  $6p^2P_{3/2}$  level cesium atoms, up to now, were carried out using incoherent light sources as optical excitation [22,23]. Guiry and Krause [22] has experimentally studied the disalignment cross section in the  $6p^2P_{3/2}$  Cs atoms in collisions with He, Ne, Ar and Xe atoms using Zeeman scanning technique. Although the study of the collisional depolarization of an excited level alkali in the gas phase has been reported, no experimental investigation of the disalignment cross section for the Cs  $J = 3/2$  atoms in collision with Kr atoms has been conducted using nanosecond pump-probe laser technique. In the experiment, a nanosecond pulse pump-probe laser technique was employed to obtain a linear polarization degree as a function of the Kr gas pressures ranging from 7 mbar to 133 mbar. This method is a direct measure of the importance of the polarization to the alignment-dependent inelastic process in alkali rare-gas collisions. Since the determination of the collisional cross sections from the experimental data requires a detailed theory of collision relaxation in the excited state, Okunevich and Perel [24] developed a theory of collisional relaxation and obtained an explicit form of the relaxation density matrix of excited alkali atoms during collision with noble gas atoms describing the mixing in the  $6p^2P_{3/2}$  level. Our results agree, within stated errors, with the theoretical results of Ref. [24].

In the following sections, we briefly describe the definition of the linear polarization in terms of alignment (state multipole) induced in the excited level by optical pumping, and discuss the systematic effects, and show rate equation analysis used to extract disalignment cross section value from the polarization spectra.

## 2. Basic description of polarization spectroscopy

In this section a basic concept of angular momentum polarization for the  $J = 3/2$  atoms and detection of atomic polarization in terms of density matrix with expansions in irreducible tensor operators in an axially symmetric systems are described. The excitation of an ensemble of atoms is achieved by an absorption of a linearly polarized light whose electric field is parallel to the  $z$  axis. The direction of light electric field defines a quantization axis for the atomic angular momentum in this case.

### 2.1. Alignment created in the $J = 3/2$ level

Here we use brief description and physical interpretation of state multipole, namely alignment. The detailed descriptions of the collisional depolarization of atomic states by thermal atom-atom collisions has been theoretically investigated in several formalisms and can be found elsewhere [25,26,5]. We consider Cs atoms in a  $^2P_{3/2}$  level undergo collisions with Kr atoms. The excited-state ensemble of  $J = 3/2$  atoms can be represented by a  $(2J + 1)^2$  density matrix  $\rho_{MM'}$  elements which can be conveniently expanded in terms of irreducible tensor components  $T_q^k$  in order to obtain explicit expressions for the angular momentum polarization. Such expansion offers an equivalent description of the distribution of  $M$  in a prepared  $J$  level. The relation between the

spherical tensor moments and the density matrix elements can be written by [20,27]

$$T_q^k(J) = \sum_{MM'} \rho_{MM'} (-1)^{k-J-M} C(JJ'k; MM'q), \quad (1)$$

where  $C(\dots)$  is a Clebsch–Gordon coefficient. Since tensors transform under rotations as spherical harmonics, the expression  $\sum_{MM'} \rho_{MM'}$  in Eq. (1) can be avoided by manipulating the tensors using angular momentum algebra. That is the shape of each tensor moment  $T_q^k$  is the same as spherical harmonic  $Y_k^q(\theta, \phi)$  [28,25].

There are in principle four axially symmetric multipole tensors  $T_q^k (q = -k \dots + k)$  in the  $J = 3/2$  level with the angular momentum distribution up to rank 3 ( $k = 2J$ ). These four axially symmetric multipoles are defined as monopole (population) for  $k = 0$ , magnetic dipole moment (orientation) for  $k = 1$ , electric quadrupole moment (alignment) for  $k = 2$ , and octupole moment for  $k = 3$ . The off-diagonal elements of  $\rho_{MM'}$  (represent coherences) contain phase information between the magnetic sublevels while the diagonal elements represent populations in the magnetic sublevels. Although there are 16 tensor components, symmetry relations can be used to reduce the number of non-zero components. Since our system is cylindrically symmetric about the quantization axis which is defined by the electric field direction of the pump laser, only  $q = 0$  components of multipoles (diagonal elements of  $\rho_{MM'}$ ) survive. All other components of  $q \neq 0$  (off-diagonal elements of  $\rho_{MM'}$ ) are zero. Thus, coherences are not generated between Zeeman sublevels in the excited level with the choice of quantization axis along the electric field direction of a linearly polarized light. Although a particular collision can generate coherences between Zeeman sublevels, these do not survive averaging over isotropic collisions with Kr atoms [29]. It is also important to note that spontaneous emission to lower levels can generate coherences, but these coherences are averaged out over the ensemble of atoms. As a result, coherences need not be considered for any theoretical and experimental modeling described in this report. Also, we consider the fact that (a) the  $6s-6p$  dipole transition can only probe the highest multipole of rank 2, and (b) linearly polarized light can only create alignment not orientation in the  $^2P_{3/2}$  level. Therefore, in this report, we define the intensity of the emitted light in terms of the zeroth component of alignment tensor  $\langle A_0 \rangle$  only. A further discussion of the cylindrically symmetric system is made in the following section.

The alignment can be defined in terms of the angular momentum quantum numbers [26,25] as

$$\langle A_0 \rangle = \sum_M |\sigma(M)|^2 \frac{[3M^2 - J(J + 1)]}{J(J + 1)}, \quad (2)$$

where  $J$  is the total angular momentum of the excited level and  $\sigma(M)$  is the cross section for excitation of the magnetic sublevels

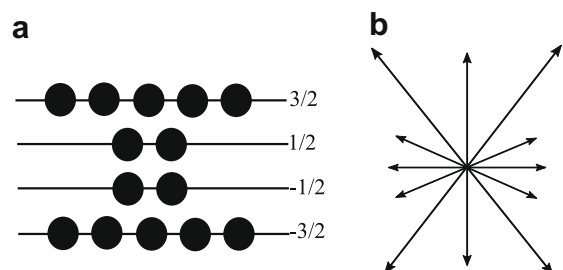


**Fig. 1.** Aligned axially symmetric system for the  $J = 3/2$  atoms diagrammatically representing (a) population distribution over the Zeeman sublevels ( $M_J$ ) and (b) angular momentum vector distribution pointing into directions of space which are allowed. Note that the net angular momentum of an aligned system is zero.

with quantum number  $M$ . Using the analogy of Greene and Zare [25], the population distribution among the magnetic sublevels for an aligned  $J = 3/2$  atom is illustrated in Fig. 1a and related angular momentum vector distributions in an aligned axially symmetric system, invariant under the reversal of  $z$  axis, in Fig. 1b. An axially symmetric system possess no net angular momentum due to the balance in the populations of the Zeeman sublevels with magnetic quantum number  $\pm M$ . Alignment provides information on the nature of the spatial distribution of angular momentum vectors and the relation to the shape of the excited level charge distribution. Using a linearly polarized light with its electric field direction along  $z$  axis transition occurs between the magnetic sublevels of the ground and excited levels with  $\Delta M = 0$ . Thus, from Eq. (2), calculated value of the alignment in the  $J = 3/2$  excited level with the absence of external perturbations is  $-4/5$ .

## 2.2. Detection of atomic polarization

Here we describe cylindrically symmetric experimental situation and the dependence of intensity of emitted light on polarization. In describing the system of geometry we utilized two space-fixed frames of reference. These are the collision (lab) frame with coordinates  $(x, y, z)$  and detector frame with coordinates  $(x', y', z')$ . Although the collision process can be generally described in the collision frame of coordinates  $(x, y, z)$ , the detection of the fluorescence is better described in a detector frame of coordinates  $(x', y', z')$ . We designated the axis of cylindrical symmetry to be the collision frame  $z$  axis. For excitation with linearly polarized light where the polarization direction of the laser  $E_1$  is parallel to the collision  $z$  axis we have cylindrical symmetry. If one chooses the detector to view along the  $z'$  direction, the polarization vector lies in the  $(x', y')$  frame and is defined as  $\hat{e}' = \hat{x}' \cos \beta + \hat{y}' \sin \beta$  where  $\beta$  is the polarization state of light. The intensity of emitted radiation  $I$  during a transition between a final level  $|f\rangle$  and an initial level  $|i\rangle$  is proportional to  $I = C \sum_f |\langle f | \hat{e}^* \cdot \vec{r} | i \rangle|^2$ . Here, the levels  $|i\rangle$  and  $|j\rangle$  describe the emission or absorption process in the collision frame, while  $\hat{e}^*$  describes the radiation in the detector frame, and  $\vec{r}$  is the coordinate of the electron. Thus, one can see that it is the transformation of  $\hat{e}^* \cdot \vec{r}$  between the detector frame and collision frame that gives the polarization and angular distribution of radiation [21]. Note that  $\hat{e}^* = \hat{e}$  and also  $\hat{e} \cdot \vec{r} = x \cos \beta + y \sin \beta$ . It is more convenient to define the intensity of emitted radiation in term of state multipoles [25,21] as

$$I(\phi, \theta, \chi) = \frac{1}{3} I_0 \left\{ 1 - \frac{1}{2} h^{(2)}(J') \langle A_0 \rangle P_2(\cos \theta) + \frac{3}{4} h^{(2)}(J') \langle A_0 \rangle \sin^2 \theta \cos 2\chi \cos 2\beta \right\}, \quad (3)$$

where  $I_0$  is the total intensity,  $\beta$  is the polarization state of light,  $(\phi, \theta, \chi)$  are Euler angles relating the collision frame to the detector frame using rotation matrices [25],  $h^{(2)}(J')$  is a geometrical quantity that depend only on the angular momentum quantum numbers of initial and final levels,  $\langle A_0 \rangle$  is the average electronic alignment in the excited level, and  $P_2(\cos \theta) = \frac{3}{2} \cos^2 \theta - \frac{1}{2}$  is the second rank Legendre polynomial. Fig. 2 shows light-matter interaction geometries. Fig. 2a describes one-photon absorption case and detecting the only linearly polarized light of the emitted radiation as obtained by a linear polaroid mounted in front of a polarization insensitive detector. It is usually more convenient to detect light at a right angle to the collision  $z$  axis so that  $\theta = \pi/2$ . It is important to notice that Eq. (3) has no dependence on the angle  $\phi$  due to cylindrical symmetry and can be re-written as

$$I(\chi) = \frac{1}{3} I_0 \left\{ 1 + \frac{1}{4} h^{(2)}(J') \langle A_0 \rangle (1 + 3 \cos 2\chi \cos 2\beta) \right\}, \quad (4)$$

where  $\chi$  is the relative angle between the  $z$  axis and the linear polarization axis of the polaroid in front of the detector. The detector in this case is in the  $xy$  plane. Since the system has cylindrical symmetry the most convenient way is to choose  $\phi$  at  $\pi/2$  as shown in Fig. 2b which illustrates that the excited level population can be probed by using a second linearly polarized light resonantly tuned to a final level. This alternative approach yields a two-photon absorption and observation of cascade fluorescence. The observed cascade fluorescence in this case is proportional to the final level population only. Detailed description of the relation between one-photon and two-photon absorption geometries is given by Refs. [30,31]. The methods of measuring  $I(\phi, \theta, \chi)$  in Eq. (3) and  $I(\chi)$  in Eq. (4) do not depend on the factors related to absorption or emission, but on geometrical angles and on the initial and final angular momenta through  $h^{(2)}(J')$ . Therefore, in order to measure the quantities such as  $I_0$  and  $\langle A_0 \rangle$  we must measure the cascade fluorescence intensities  $I(\chi)$  at two settings of the polaroid in front of detector or at two settings of the probe polarization angle  $\chi$  (as in the case of this work). We designated the probe polarization at two settings as  $I_{\parallel}$  when  $\chi = 0$  and  $I_{\perp}$  when  $\chi = \frac{\pi}{2}$ , as seen in Fig. 2b. From these settings we obtain two intensity measurements  $I_{\parallel}$  when the polarization direction of the probe laser is along  $z$  axis and  $I_{\perp}$  when the

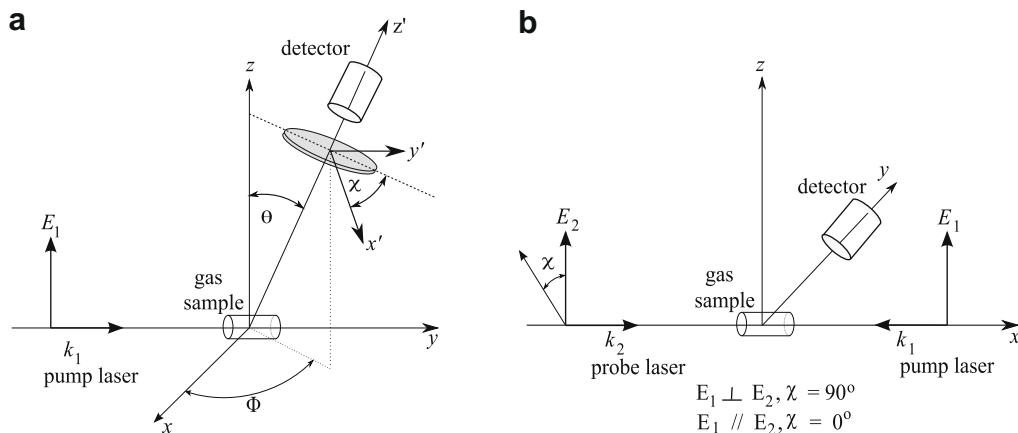


**Fig. 2.** Light-matter interaction geometry representing (a) one-photon absorption: the detector in this case detects only linearly polarized light as may be obtained by a linear polaroid mounted in front of a polarization insensitive detector, (b) two-photon absorption: the detector in this case detects cascade fluorescence from a final level which is proportional to probe population only.

polarization direction of probe laser is perpendicular to  $z$  axis. Thus, the measured intensities of cascade fluorescence  $I_{\parallel}$  and  $I_{\perp}$  can be defined as

$$I_{\parallel} = \frac{I_0}{3} \left\{ 1 + h^{(2)} \langle A_0 \rangle \right\}$$

and

$$I_{\perp} = \frac{I_0}{3} \left\{ 1 - \frac{1}{2} h^{(2)} \langle A_0 \rangle \right\}.$$

From the measured  $I_{\parallel}$  and  $I_{\perp}$  quantities we obtain the degree of linear polarization defined by

$$P_L = \frac{I_{\parallel} - I_{\perp}}{I_{\parallel} + I_{\perp}}. \quad (5)$$

Our experimental geometry is designed in such a way that the propagation directions of the pump and probe lasers are perpendicular to the axis of symmetry. For the  $6p^2P_{3/2} \rightarrow 10s^2S_{1/2}$  transition by linearly polarized light,  $h^{(2)}(\frac{3}{2}, \frac{1}{2})$  has a value of  $-5/4$  [25]. Substituting  $I_{\parallel}$ ,  $I_{\perp}$ , and  $h^{(2)}$  value into Eq. (5), we can define  $P_L$  in terms of alignment  $\langle A_0 \rangle$  as

$$P_L = \frac{-15 \langle A_0 \rangle}{16 - 5 \langle A_0 \rangle}, \quad (6)$$

which may be inverted to define alignment in terms of measured  $P_L$  as

$$\langle A_0 \rangle = \frac{16 P_L}{5 P_L - 15}. \quad (7)$$

The polarization degree  $P_L$ , determined without and with the presence of buffer gas at various pressures, is the main quantity measured in the experiment. It is important to point out that an absolute intensity ratio of the signals is sensitive only to the relative polarization directions of the lasers. Although the measured linear polarization degree generally depends on systematic factors such as stray magnetic or electric fields, collisions, hyperfine depolarization in the excited level, such effects are mitigated in the present experiment by using a broadband nanosecond pulse dye lasers and by adjusting the temporal overlap of the pulses to about 1 ns. Further discussion of these factors is made in a later section of this report. Therefore, any variations of the laser intensities with experimental factors such as absorbing medium density, fluorescence background, sensitivity of the gated boxcar integrator, collectively do not affect the intensity ratio.

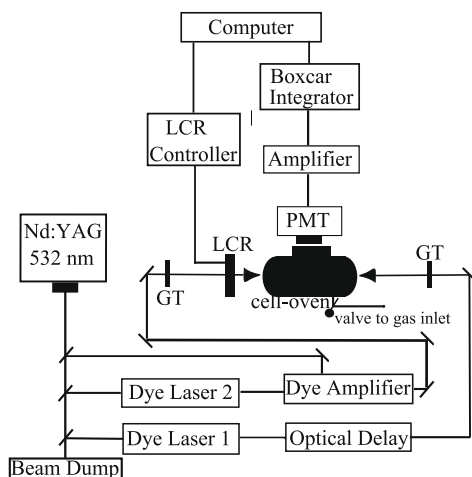


**Fig. 3.** A schematic diagram of the experimental apparatus. GT, Glan–Thompson prism polarizer; LCR, liquid-crystal variable retarder; PMT, photo-multiplier tube.

### 3. Experimental procedure and measurements

The schematic diagram of the experimental apparatus is shown in Fig. 3. In general, a two-photon two-color transition is induced between the atomic ground level and a selected higher-lying excited level. We used two tunable pulse dye lasers for that purpose. The wavelength of the first laser is at 852.1 nm resonance of the  $J = 3/2$  excited level and the wavelength of the second laser is at 603.4 nm. We used the second harmonic generator of a pulsed neodymium-doped yttrium aluminum garnet (Nd:YAG) solid state laser operating at 20 Hz with an average power of 2 W in order to pump two dye lasers. The beam of these home-built pulse dye lasers are directed collinearly but in opposite directions into the interaction region of the cell. Dye laser oscillators are of the grazing incidence Littman–Metcalf cavity design and the outputs of both are highly linearly polarized. Dye laser 1 (pump laser), equipped with a dye circulating system to maintain the power stability around 0.03 mW, operates at the fixed wavelength of the Cs D2 line at 852 nm and has a bandwidth of approximately  $0.9 \text{ cm}^{-1}$ . The output power of dye laser 2 (probe) from the oscillator is increased by about a factor of 10 using a dye amplification system which generates an average power of about 2 mW. The probe laser has a bandwidth of approximately  $0.2 \text{ cm}^{-1}$  and its oscillator produces light for the  $6s^2P_{3/2} \rightarrow 10s^2S_{1/2}$  transition at 603.4 nm. The wavelengths of the lasers are measured using a Coherent wavemeter with a precision of 0.001 nm. Glan–Thompson prism polarizers with extinction ratios of better than  $10^{-5}$  is used in lasers paths. A temperature-controlled liquid crystal variable retarder (LCR) with an extinction ratio of  $10^{-4}$  was used in the probe beam path in order to electronically vary the linear polarization direction of the light to be parallel or perpendicular to that of pump laser. Polarization switch of the LCR was achieved by applying the necessary voltage to the retarder via a computer-controlled liquid crystal digital interface. The Pyrex cell containing cesium has an adjustable valve and the cell system is connected to the buffer-gas cylinder for slow introduction of the gas into the cell. A resistively heated non-magnetic cylindrical aluminum oven was used to heat the cell. The oven was wrapped with an aluminum oxide blanket to maintain the temperature better than  $\pm 0.01 \text{ }^\circ\text{C}$  via a temperature controller.

The intensities of the cascade fluorescence from the  $9p^2P_{1/2}$  level to the ground  $6s^2S_{1/2}$  level were recorded at 361.73 nm by using a UV sensitive photomultiplier tube (PMT). A combination of inter-

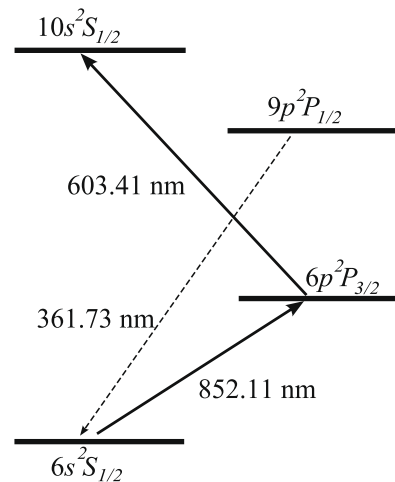


**Fig. 4.** Some of the important transitions and their corresponding wavelengths are shown in solid line, the cascade fluorescence channel observed in the experiment is shown in dotted line.

ference and color glass filters were used in front of the PMT in order to remove background due to scattered and atomic resonance fluorescence. Illustration of the excitation scheme with corresponding wavelengths [32,33] is shown in Fig. 4. The PMT was located at right angles to the propagation directions of the lasers. All the cables used in the experiment were electrically shielded and the optical table was grounded in order to eliminate electronic pickup and noise on the observed signal. The output of the PMT signal was amplified using a two stage amplifier and processed in a boxcar integrator/averager with a 60-ns gate-width, opened after a 1 ns delay following the laser pulses, operating in a sample-and-hold mode, where the average single-shot level within the detection gate is digitized. Our typical signal size is about  $10^3$  photons for each laser pulse. The digitized signals were stored on a computer using a LabVIEW program while monitoring the size of the signal within the gate in real time using a digital oscilloscope operating at 500 MHz.

### 3.1. Discussion of systematic effects

For atoms with non-zero nuclear spin, the total angular momentum  $\vec{J}$  of the ensemble couples to the nuclear spin moment  $\vec{I}$  to produce a space-fixed  $\vec{F}$ , where  $\vec{F}$  is a total angular momentum.  $\vec{J}$  will then precess about  $\vec{F}$  so that the initially prepared space-fixed frame is altered. The precession affects all state multipoles. This effect has been explained in the study of angular momentum alignment resulting from optical pumping and photodissociation [34,26]. In the case of  $^{133}\text{Cs}$ , the coupling of nuclear spin  $I = 7/2$  with  $J = 3/2$  introduces an oscillating time dependence in the alignment tensor moment and changes the amount of alignment optically induced in the excited level. The time scale of the coupling between the nuclear spin  $\vec{I}$  and angular momentum  $\vec{J}$  is important to determine the amount of effect on the alignment. Time evolution of the alignment under the influence of the hyperfine structure can be described as  $\langle A_0(t) \rangle = \langle A_0 \rangle g^{(2)}(t)$ , where  $g^{(2)}$  is the alignment hyperfine depolarization coefficient [35,36] which decrease from its maximum value of 1 at  $t = 0$  and begin to oscillate between the values of 1 and  $-1$  as  $t > 0$ . However, if the temporal overlap time of the two pulses can be adjusted in such a way that the overlap time is smaller than the inverse of the highest hyperfine frequency component, one can possibly freeze out the electronic alignment in the excited level. That is, the excited  $J = 3/2$  atoms promoted to the final  $10s^2S_{1/2}$  level by the two-photon double-resonance excitation before the hyperfine precessional motion can be taken place. We have made a special effort on constructing an optical delay to control the arrival time of the pump laser to the interaction region of the cell. The overlap time of our pump-probe lasers is made to about  $\sim 1$  ns which is smaller than the hyperfine precession time of 3.5 ns in the excited level. Therefore, we do not expect significant nuclear hyperfine depolarization during the overlap time of the pulse lasers.

We have also checked for the existence of external perturbations such as radiation trapping, the influence of laser power and temperature dependence on the measured polarization spectrum. Due to the short temporal overlap time of the pulses compared to the radiative lifetime of the excited level ( $\tau = 33$  ns), approximately 3% of the excited atoms will have radiatively decayed during the pulse. Therefore, we expected radiation trapping has a negligible effect on the excited level. Also, the Earth's magnetic field was cancelled by using mu-metal surrounding the cell-oven system. In order to be assure that the laser powers and Cs cell temperature were not modifying the measured polarization degree during the two-photon double-resonance excitation, measurements of laser power and temperature dependence to the polarization spectra were performed. Both results were found to be independent of laser power and Cs density. In the absence of any

**Table 1**

Table shows the calculated and the measured values of alignment in the  $^2P_{3/2}$  level and a linear polarization for the  $6s^2S_{1/2} \rightarrow 6p^2P_{3/2} \rightarrow 10s^2S_{1/2}$  transition.

$\langle A_0 \rangle_{cal.}$	$\langle A_0 \rangle_{meas.}$	$(P_L)_{cal.}$	$(P_L)_{meas.}$
-0.8	-0.81 (0.04)	60%	60.5 (2.5)%

depolarizing effects, linear polarization  $P_L$  is 0.6 (60%). Measurements of the linear polarization spectra obtained for the  $6s^2S_{1/2} \rightarrow 6p^2P_{3/2} \rightarrow 10s^2S_{1/2}$  transition confirm that  $J = 3/2$  level has no external perturbations that measurably alter the alignment in the  $6p^2P_{3/2}$  level. The measured linear polarization degree is found to be 60.5 (2.5)%. We summarized in Table 1 calculated values, uses Eqs. (2) and (6), and measured values of alignment and linear polarization for the  $J = 3/2$  level alkali.

### 3.2. Disalignment cross section from the rate equation analysis

Although selective excitation to the Zeeman sublevels  $M_j = \pm 1/2$  of the  $6p^2P_{3/2}$  level can be achieved by a linearly polarized pump laser according to the selection rule  $\Delta M = 0$ , the excited Cs atoms and the ground level Kr atoms collisionally mix the population in the magnetic sublevels. As a result, population can be transferred to all magnetic sublevels ( $N_{\pm 1/2}$ ,  $N_{\pm 3/2}$ ). The mixing among the  $M_j = \pm 1/2$ ,  $\pm 3/2$  magnetic sublevels reduces the amount of average electronic alignment produced in the excited level. The population variations among the Zeeman sublevels can be conveniently expressed by a simple theoretical model using the rate equations analysis [37,26] as

$$\begin{aligned} \dot{N}_{1/2} &= -(\gamma + \Gamma_1 + \Gamma_2)N_{1/2} + (\Gamma_1 + \Gamma_2)N_{3/2} + \Gamma_p, \\ \dot{N}_{3/2} &= -(\gamma + \Gamma_1 + \Gamma_2)N_{3/2} + (\Gamma_1 + \Gamma_2)N_{1/2}, \end{aligned}$$

where  $\Gamma_p$  is the pump pulse rate. Here we have used  $N_{1/2} = N_{-1/2}$  and  $N_{3/2} = N_{-3/2}$ , applicable to an electronically aligned level. The laser intensity profile was modeled using a square pulse shape. Other pulse shapes may be used and lead to the same polarization results [6,38,7]. The time dependent total population density and the alignment in the excited level can be defined by

$$N(t) = 2\Gamma_p P_b \quad (8)$$

and

$$\langle A_0(t) \rangle = -\frac{8}{5}\Gamma_p P_a, \quad (9)$$

where  $P_b = \frac{1}{\gamma}(1 - e^{-\gamma t})$  and  $P_a = \frac{1}{\gamma_a}(1 - e^{-\gamma_a t})$ . We define  $\gamma_a = \gamma + (2\Gamma_1 + 2\Gamma_2)$  as the rate at which the alignment is altered due to the collision between the Cs and Kr atoms,  $\gamma$  is the radiative decay rate, and  $(2\Gamma_1 + 2\Gamma_2)$  is the total collisional decay rate which is defined to be  $\Gamma$ . Since  $\Gamma_p$  in Eqs. (8) and (9) cancels out when the intensity ratio is taken using the linear polarization expression, it is not shown in the following derivations. The population densities in the  $M = \pm 1/2, \pm 3/2$  sublevels in terms of total population and alignment are defined as

$$N_{1/2}(t) = \frac{N(t)}{4} - \frac{10}{32}\langle A_0(t) \rangle \quad (10)$$

and

$$N_{3/2}(t) = \frac{N(t)}{4} + \frac{10}{32}\langle A_0(t) \rangle. \quad (11)$$

These population densities can be re-written in terms of  $P_a$  and  $P_b$  as

$$N_{1/2}(t) = (P_b + P_a)/2, \quad (12)$$

$$N_{3/2}(t) = (P_b - P_a)/2. \quad (13)$$

Thus, the measured signals, integrated over the temporal overlap time of the pulses, can be written in terms of  $P_a$  and  $P_b$  as

$$I_{\parallel} = \frac{1}{6} \int_0^T P_b dt + \frac{1}{6} \int_0^T P_a dt, \quad (14)$$

$$I_{\perp} = \frac{1}{6} \int_0^T P_b dt - \frac{1}{12} \int_0^T P_a dt. \quad (15)$$

Substituting Eqs. (14) and (15) into Eq. (5), a linear polarization can be expressed in terms of the depolarization cross section and the pressure of the buffer gas as

$$P_L = \frac{3Z}{4+Z}, \quad (16)$$

where

$$Z = \frac{\gamma}{\gamma_a} \left[ \frac{1 - \frac{1}{\gamma_a T} (1 - e^{-\gamma_a T})}{1 - \frac{1}{\gamma T} (1 - e^{-\gamma T})} \right]. \quad (17)$$

In Eq. (17),  $\gamma_a$  is defined to be  $\gamma + \Gamma$ , and

$$\begin{aligned} \Gamma &= \rho_{\text{Kr}} k_2 \\ &= \rho_{\text{Kr}} \sigma_2 \bar{v}_{\text{CsKr}} \\ &= \frac{p}{kT} \cdot k_2, \end{aligned} \quad (18)$$

where  $k_2$  is the disalignment rate coefficient,  $p$  is the buffer gas pressure,  $kT$  is the thermal energy constant, and  $\sigma_2$  is the disalignment cross section. We assumed that  $k_2 = \langle \sigma_2 v \rangle$ , and  $\langle \sigma_2 v \rangle$  may be factored so that  $k_2 = \sigma_2 \langle v \rangle$ . In Eq. (18), we denoted  $\langle v \rangle$  as  $\bar{v}_{\text{CsKr}}$  which is the average velocities of the colliding Cs–Kr atoms over the Maxwell–Boltzmann distribution of relative velocities at the operating cell temperature.

Eq. (16) provides the connection between the experimentally measured linear polarization degree  $P_L$  in relation to the krypton gas pressure  $p$  and the disalignment cross section  $\sigma_2$ . Thus, the disalignment cross section from the measured linear polarization spectra at Kr gas pressures ranging from 7 mbar to 133 mbar was extracted. Rate equation analysis of the  $6p^2P_{3/2}$  level population was made by modeling the laser pulse temporal profiles as square pulses. The pulse width for both lasers was measured to be approximately 6.5 ns using an ultrafast photodetector with 0.2 ns rise-time. The result of the weighted non-linear least-squares fit to the data from the Statistical Analysis Software (SAS) is illustrated

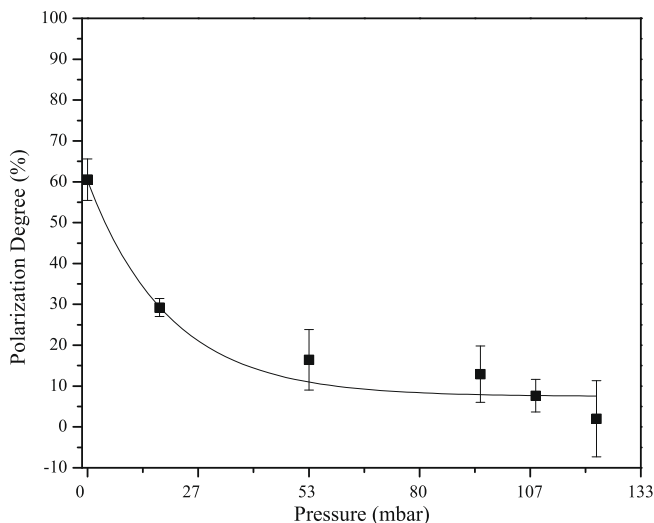


Fig. 5. Non-linear least square fit of the linear polarization spectrum for the two-photon double-resonance  $6s^2S_{1/2} \rightarrow 6p^2P_{3/2} \rightarrow 10s^2S_{1/2}$  transition.

Table 2

Disalignment cross section ( $\sigma_2$ ) of the  $6p^2P_{3/2}$  Cs atom in collision with Kr buffer gas is listed.

$\sigma_2$ ( $\text{\AA}^2$ )	Reference
294 (45)	This work
311	[24]

in Fig. 5. The error bars indicate one standard deviation. The disalignment cross section, a fitting parameter that is resulted from the weighted non-linear least-squares fitting of the experimental results using Eq. (16), is summarized in Table 2 together with the theoretical value by Okunevich and Perel [24].

## 4. Conclusions

We present in this paper results of a two-photon two-color polarization spectroscopy approach to measurement of excited-state alignment depolarization cross section. In the experiment, alignment is optically induced from a linearly polarized pump laser. Then, the linear polarization of the  $6s^2S_{1/2} \rightarrow 6p^2P_{3/2} \rightarrow 10s^2S_{1/2}$  transitions was measured. The measured linear polarization degree is found to be independent of the laser powers, temperature, and variation in the intensity of the fluorescence signal. Depolarization in the cesium excited level in collision with ground level Kr atoms is evident on the measurement of polarization spectrum. From the measurements, the disalignment cross section for collisionally induced mixing within the  $^{133}\text{Cs}$   $6p^2P_{3/2}$  level is obtained. Our result is in good agreement with the theory [24] within the error limits.

## Acknowledgement

We would like to thank Professor Mark Havey from Old Dominion University for valuable discussions. We gratefully acknowledge the financial support of the Research Corporation under the Grant No. CC7133.

## References

- [1] H. Kaupp, H.-P. Didra, C. Kramer, M. Baumann, Z. Phys. D 27 (1993) 307.
- [2] M.L. Costen, K.G. McKendrick, J. Chem. Phys. 122 (2005) 164309.
- [3] M.L. Costen, H.J. Crichton, K.G. McKendrick, J. Chem. Phys. 120 (2004) 7910.
- [4] S.B. Bayram, S. Kin, M.J. Welsh, J.D. Hinkle, Phys. Rev. A 73 (2006) 042713.
- [5] W.E. Baylis, in: W. Hanle, H. Kleinpoppen (Eds.), Progress in Atomic Spectroscopy Part B, Plenum, New York, 1979.
- [6] L. Cook, D.A. Olsgaard, M.D. Havey, A. Sieradzian, Phys. Rev. A 47 (1993) 340.
- [7] R. Lasell, S.B. Bayram, M.D. Havey, D.V. Kupriyanov, S.V. Subbotin, Phys. Rev. A 56 (1997) 2095.
- [8] T.H. Wong, P.D. Kleiber, Phys. Rev. A 57 (1998) 2227.
- [9] L.B. Zhao, A. Watanabe, P.C. Stancil, M. Kimura, Phys. Rev. A 76 (2007) 022701.
- [10] J. Weiner, V.S. Bagnato, S. Zilio, P.S. Julienne, Rev. Mod. Phys. 71 (1999) 1.
- [11] D. Leibfried, R. Blatt, C. Monroe, Rev. Mod. Phys. 75 (2003) 281.
- [12] T.F. Gallagher, Rydberg Atoms, Cambridge University Press, Cambridge, 1994.
- [13] A. Walz-Flannigan, J.R. Guest, J.-H. Choi, G. Raithel, Phys. Rev. A 69 (2004) 063405.
- [14] K.R. Overstreet, A. Schwettmann, J. Tallant, J.P. Shaffer, Phys. Rev. A 76 (2007) 011403(R).
- [15] E.A. Brinkman, D.R. Crosley, J. Phys. Chem. A 108 (2004) 8084.
- [16] U. Levy, C.-H. Tsai, L. Pang, Y. Fainman, Opt. Lett. 29 (2004) 1718.
- [17] V.M. Datsyuk, I.M. Sokolov, D.V. Kupriyanov, M.D. Havey, Phys. Rev. A 77 (2008) 033823.
- [18] D. Schurig, J.B. Pendry, S.R. Smith, Opt. Exp. 14 (2006) 9794.
- [19] A.G. Suits, R.L. Miller, L.S. Bontuyan, P.L. Houston, J. Chem. Soc. Faraday Trans. 89 (1993) 1443.
- [20] U. Fano, Rev. Mod. Phys. 29 (1957) 74.
- [21] U. Fano, J.H. Macek, Rev. Mod. Phys. 45 (1973) 553.
- [22] J. Guiry, L. Krause, Phys. Rev. A 14 (1976) 2034.
- [23] J. Fricke, J. Haas, E. Lüscher, Phys. Rev. 163 (1967) 45.
- [24] A.I. Okunevich, V.I. Perel, Sov. Phys. JETP 31 (1970) 356.
- [25] C.H. Greene, R.N. Zare, Ann. Rev. Phys. Chem. 33 (1982) 119.
- [26] K. Blum, Density Matrix Theory and Applications, Plenum, New York, 1981.

- [27] J. Macek, I.V. Hertel, *J. Phys. B* 7 (1974) 2173.
- [28] C.A. Taatjes, S. Stolte, *J. Chem. Soc. Faraday Trans. 10* (1993) 1551.
- [29] M.D. Havey, Private communication.
- [30] A.C. Kummel, G.O. Sitz, R.N. Zare, *J. Chem. Phys.* 85 (1986) 6874.
- [31] A.C. Kummel, G.O. Sitz, R.N. Zare, *J. Chem. Phys.* 88 (1988) 6707.
- [32] A.A. Radzig, B.M. Smirnov, *Reference Data on Atoms, Molecules, and Ions*, Springer-Verlag, New York, 1985.
- [33] K.-H. Weber, C.J. Sansonetti, *Phys. Rev. A* 35 (1987) 4650.
- [34] R.N. Zare, *Angular Momentum: Understanding Spatial Aspects in Chemistry and Physics*, Wiley, New York, 1988.
- [35] E. Arimondo, M. Inguscio, P. Violino, *Rev. Mod. Phys.* 49 (1977) 31.
- [36] N. Andersen, K. Bartschat, *Polarization Alignment and Orientation in Atomic Collisions*, Springer-Verlag, New York, 2001.
- [37] K. Blushs, M. Auzinsh, *Phys. Rev. A* 69 (2004) 063806.
- [38] R. Lasell, D.A. Olsgaard, S.B. Bayram, M.D. Havey, D.V. Kupriyanov, *Phys. Rev. A* 58 (1998) 779.